Optimal Bimodal Pore Networks for Heterogeneous Catalysis

Stefan Gheorghiu and Marc-Olivier Coppens
Dept. of Chemical Technology, Delft University of Technology, Julianalaan 136, 2628 BL Delft, The Netherlands

DOI 10.1002/aic.10076
Published online in Wiley InterScience (www.interscience.wiley.com).

A practical problem in the rational design of a heterogeneous catalyst is to optimize its structure at all scales. By optimizing the large-pore network of a bimodal porous catalyst with a given nanoporosity (for example, zeolite or mesoporous catalyst) for the yield of diffusion-limited first-order reactions, it is found that catalysts typically benefit from a hierarchical pore network with a broad pore-size distribution. When comparing the performance of the optimal structures to that of self-similar, fractal-like pore hierarchies, it is found that the latter can be made to have the same effectiveness factor as the optimal ones, suggesting that fractal-like catalysts operate very near optimality, even if their structure is considerably different from that of the true optima. This is useful, because fractal-like structures have the advantage of being organized in a modular, natural way, potentially easy to reproduce by templating. © 2004 American Institute of Chemical Engineers
AIChE J, 50: 812–820, 2004
Key words: optimization, catalysis, porous media, fractals, bimodal catalysts

Introduction

A huge scientific effort is currently being witnessed, aimed at the design and synthesis of novel nanoporous materials with controlled porosity, for applications ranging from catalysis, to fuel cells, batteries, and solar cells (Kresge et al., 1992; Zhao et al., 1998; Sun et al., 2001a). Recently, research is being extended to the development of bimodal, "multistructured" materials with a controlled pore network structure at multiple length scales (see, for example, Sun et al., 2003). On the theoretical side, reaction, and diffusion in catalysts with a bimodal pore or particle-size distribution has been studied extensively (Hegedus and Pereira, 1990; Loewenberg, 1994; Andrade et al., 1995; Dogu, 1998). In catalysis, such materials could combine a desirable high internal catalyst surface along narrow nanopores with facile molecular transport through broad "highways" leading to and from these pores.

Inspired by the increasing capabilities to synthesize advanced materials with tailor-made pore networks, with self-assembly techniques, such as surfactant templating (Sun et al., 2001b), this article addresses the optimal structure of bimodal, multistructured porous catalysts, with a *given constant nanoporosity* (imposed by the use of a zeolite or other microporous material that the catalyst particles are prepared from), and a *variable* large-pore network which we aim to optimize. In this article, we depart from the established approach to the optimization of multistructured catalysts (for example, Keil 1999), where the main targets of the optimization are typically the *micropore* radius and porosity, whereas the structure of the large-scale pore network is considered of lesser interest.

Beyond pore-network optimization, this study compares the performance of the optimized large-pore network to that of pore networks that are either fractal-like or uniform (that is, bidisperse, with two distinct, constant pore sizes). The interest for such a comparison lies in the fact that both fractal-like and bidisperse pore structures are attractive solutions for catalysis, which have been studied extensively in the past, and for which novel synthesis methods are becoming available. Structures with a fractal pore-size distribution were advocated as high-performance catalysts by several researchers (Pfeifer and Avnir, 1983; Avnir et al., 1984; Villermaux et al., 1987). Later, computational and analytical studies of diffusion and reaction

Correspondence concerning this article should be addressed to M.-O. Coppens at m.o.coppens@tnw.tudelft.nl.

in fractal pore networks (Coppens and Froment, 1997; Gavrilov and Sheintuch, 1997) showed that catalysts with a self-similar pore-size distribution ranging from a finite smallest to a largest length scale (that is, a finite fractal range), may indeed increase the yield compared to catalysts with a narrow pore-size distribution, in the case of diffusion-limited processes. Other studies on catalysts with a fractal pore network (Giona et al., 1996; Sheintuch, 2000), or a fractal internal surface (Mougin et al., 1996; Sapoval et al., 2001), also suggest a lower sensitivity to deactivation as compared to other structures.

There are fundamental rationales why fractal-like pore networks could be optimal, and why the structure of networks at the meso– to macroscopic scale may be very relevant. First, Bejan and coworkers have shown that hierarchical, self-similar trees of channels are optimal to cool uniform heat generators (Bejan, 1996), of relevance to the cooling of ICs, as well as to maximize fluid flow in porous structures (Bejan and Errera, 1997). The nature of these optima was justified by Bejan (2000), based on principles from irreversible thermodynamics. Second and perhaps related to this, hierarchical, fractal trees are omnipresent in nature. The objects of this investigation mimic living systems, where slow diffusion of nutrients and oxygen through tissue is accompanied by fast distribution through a network of blood or air vessels. Because nature does not squander resources, it is likely that its "bioreactors" (lungs, kidneys, cells in tissue, and so on) are performing diffusion-reaction tasks in an optimal way. By analyzing the optimal catalyst geometry, we may make a modest step forward in understanding if and why this is so. In return, one can learn from nature's own designs to improve technology, not only at the microscale, but also all the way up to the macroscopic scale where the design of more efficient reactors can contribute to process intensification.

Optimal bimodal porous media for catalysis

A nanoporous catalyst particle (for example, zeolite, amorphous ordered, or disordered silica or alumina) is treated as an effective medium with a known, effective diffusivity D_e for the reacting species A, a density ρ, and a first-order, isothermal reaction A $\rightarrow$ B with known intrinsic rate constant k. The effective-medium approximation for the nanoporous "flesh" is justified far enough from the percolation threshold. To reduce diffusion limitations, a network of large pores is drilled into the nanoporous pellet. This drilling does not have to be taken literally; small nanoporous particles could also be *assembled* into larger pellets. This assembly creates "highways" that serve as fast-transport channels (each pore i having a diffusivity $D_{0i} \gg D_e$), but at the same time removes reactive material, potentially lowering the overall yield. The tradeoff between increasing access to catalyst sites and lowering the amount of active material hints at the existence of a network with optimal porosity and geometry. In this section of the study, the geometry is optimized numerically, by adapting the network structure with the goal of maximizing the production of B in a catalyst pellet with a given constant volume. Both the amount of nanoporous material (that is, pellet porosity) and its spatial distribution within this volume are subject to optimization.

This simplified model of a pellet is meant only as a tool to search for governing principles and guidelines for the general optimization of reaction-diffusion processes, and yields valuable insight into the rational design of novel porous materials. Although a first-order reaction is usually an oversimplification, future generalizations, such as multicomponent diffusion and complex reaction networks with arbitrary kinetics may use the same computational framework.

A two-dimensional (2-D) model with a square symmetry is used to represent a catalyst pellet. No *a priori* assumptions are made about the geometry of the high-diffusivity channel network, except that channels are straight, perpendicular to the square sides, and have a fixed cross section as they cross the entire pellet. Although the pellet has an 8-fold symmetry, there is no mathematical reason why the optimal networks should have the same high degree of symmetry. For very simple structures (for example, 2×2 pores), we found that optimal networks may have a lower degree of symmetry (for example, 2-fold or 4-fold) for strong diffusion limitations. However, calculations also showed that already for a moderate number of pores, the optimal networks are highly symmetric. Therefore, in the rest of this study, we only search for solutions with the full symmetry of the square. The use of symmetry saves computational time by orders of magnitude, by reducing the number of independent variables in the optimization scheme, which also has positive effects on the rate of convergence and on the reliability of the global optimum. The assumption of 8-fold symmetry is preserved throughout this study, which allows for a consistent comparison of the performance of networks with different geometries.

A high-performance finite-element solver for MATLAB (FEMLAB 2.2) was used to compute the concentration field. The complete 2-D solution to the reaction-diffusion partial differential equation within reactive regions, is matched to the solution of the diffusion equation in the high-diffusivity channels across all channel walls, and boundary conditions are imposed at the square sides

$$\begin{aligned} &D_e\nabla^2 c(x, y) - k\rho c(x, y) = 0 && \text{in the nanoporous solid} \\ &D_{0i}\nabla^2 c(x, y) = 0 && \text{in the } i\text{-th large pore} \\ &c(x, 0) = c(x, L) = c(0, y) \\ &\quad = c(L, y) = C_0 && \text{at the boundaries} \end{aligned} \tag{1}$$

Note that the nanopores and the large pores must be separated by at least one order of magnitude in size, in order for the nanoporous material to be safely considered as an effective medium with diffusivity D_e. This is typically a reasonable assumption. The production is given by

$$Y = \int_0^L \int_0^L k\rho(x, y)c(x, y)dxdy \tag{2}$$

where $\rho(x,y)=\rho$ inside "flesh" regions and zero in the large pores. The yield is then considered as the objective function for a geometric optimization algorithm.

The position and width of all channels are optimized simultaneously, which is equivalent to a simultaneous optimization of the pellet porosity and spatial structure. This kind of problem poses significant computational difficulties. Because of the rather large number of independent variables, and the presence of many local minima (suboptimal configurations), usual opti-

mization algorithms may fail to find the global optimum. To overcome these difficulties, a combination of genetic algorithms and classic line search algorithms was used. Together with simulated annealing methods, genetic algorithms are currently considered one of the most efficient strategies for searching for global optima in high-dimensional variable spaces (Goldberg, 1989). The position and size of the network channels are encoded as a real-valued n-dimensional vector, called a "chromosome". First, a catalog of random chromosomes is assembled, to form a starting "gene pool" of possible candidates for the optimal network. The candidates are sorted according to their respective yields. The search for the optimum proceeds by selecting "parents" from the pool of candidates (usually favoring individuals with high yields), and computing a new generation of chromosomes, via two classes of operations: "mutations" and "crossovers". Mutations correspond to random changes in a chromosome, whereas crossovers are interpolations between the parent chromosomes. At every generation, the resulting networks are sorted by yield, and the worst performing individuals are discarded. Through the quasi-random selection of parents, the algorithm explores the entire variable space simultaneously, and is capable of singling out a good candidate for the global optimum after a moderate number of iterations. In the next stage of the optimization scheme, this candidate is taken as the initial guess for a Levenberg-Marquardt line search algorithm, which ultimately converges to the optimal network configuration.

This approach differs significantly from previous studies, in several respects. First, this is to our knowledge the first attempt of global geometric optimization of network geometry for catalysis. Second, such pellet models are usually solved by network approximations in which reaction only occurs on the *channel walls* (for example, Mougin et al., 1996; Gavrilov and Sheintuch, 1997). In this study, the channel walls are permeable, which leads to concentration gradients in the microporous "flesh" between the channels, and even allows for cross-flow between two neighboring channels through the adjacent wall. This has an important effect on the pellet yield and the optimal distribution of active material. This effect cannot be seen in simple models with reaction on the walls, which justifies the use of a computationally expensive method, such as FEM to calculate the full 2-D concentration field. Finally, our optimization strategy is also complementary to that of Morbidelli et al. (2001), who considered the catalyst support as given ($D(x,y)=D_e$ constant and fixed), but with a variable distribution of active sites on the support ($k=k(x,y)$), which is optimized. In our simulations, k is fixed, whereas the *geometry* of the catalyst support is optimized.

It is convenient to define a Thiele modulus

$$\phi^* = L\sqrt{k\rho/D_e} \tag{3}$$

which depends on the effective diffusivity in the nanoporous flesh. The "real" Thiele modulus of the pellet, ϕ, will typically be smaller than ϕ^* because of fast transport through the large pores. There is no simple way of expressing ϕ, because it involves the network geometry and the details of transport in the large pores in a nontrivial fashion, but its value can be approximated based on, for example, the effective medium approach (Sahimi et al., 1990).

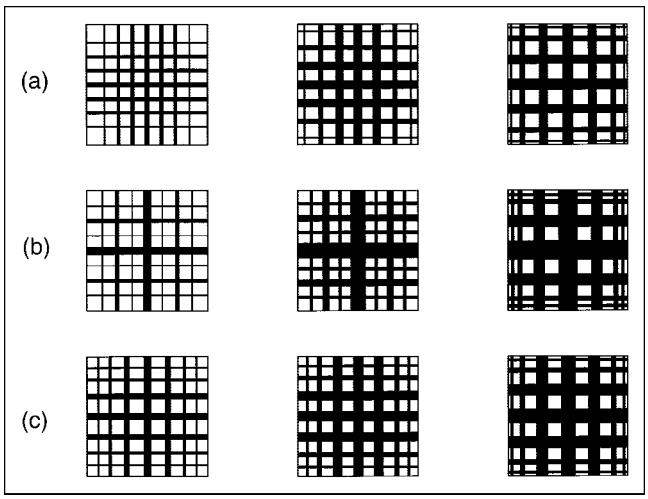

Figure 1. Optimal geometry of square networks with 7 × 7 pores.

Pores are black, microporous catalytic support is white. From left to right, $\phi^*=10$, 31.6, 100. (a) Molecular diffusion in the large pores, $D_0/D_e=10^2$. (b) Knudsen diffusion in the large pores, $D_K/D_e=10^3$. (c) Intermediate diffusion regime with realistic process parameters: $D_0/D_e=2\times10^2$, $D_K/D_e=2\times10^3$. ϕ^* is defined in Eq. 3.

It is expected that the details of diffusion in the large pores are determinant for the shape of the optimal networks. Therefore, we first consider the extremes of pure molecular diffusion and Knudsen diffusion as the dominant transport mechanism in the large pores, and later a more realistic Bosanquet-type interpolation between the two. Beyond 1 μm in pore size, pressure-driven flow should typically be included. The current framework does not consider flow, because for an isomerization A $\rightarrow$ B there are no appreciable pressure gradients, so diffusion dominates at all scales.

The molecular diffusion regime

The assumption that channel transport is dominated by molecular diffusion is justified for macropores, that is, pores wider than approximately 50 nm (the actual crossover value where Knudsen diffusion becomes negligible depends on pressure and temperature). In this case $D_{0i}=D_0$, the same for all pores.

Typical optimal configurations with 7×7 large pores are shown in Figure 1a for $D_0/D_e=100$ and three different values of ϕ^*(Eq. 3). As expected, the porosity of optimal networks increases with increasing ϕ^*. For all ϕ^* values, the optimal networks have a nonuniform spatial distribution of catalyst material. Instead of a mono- or bidisperse pore-size distribution, the optimal distribution is broad, and wider channels drain into thinner ones. Equally apparent is a radial porosity gradient within the pellet. For fast reactions (large ϕ^*), there is a striking pattern emerging in the organization of outside layers. Channels tend to concentrate in this area, with the net effect of increasing the surface area exposed to the high concentration of reactant at the pellet surface. Simultaneously, the channel size is smallest in this area, so the porosity is kept in check, and valuable productive catalytic material is not lost. Thus, the optimal configuration for fast reactions is an "eggshell" geometry, where the bulk of the production is concentrated in the pellet skin, a well known fact in chemical reaction engineering

(Froment and Bischoff, 1990). Both porosity and its spatial allocation are equally relevant for optimization.

When comparing optimal networks having the same modulus ϕ^*, but different macropore diffusivity D_0, it is found that high D_0/D_e values accentuate the nonuniformity of the network, both in size and position of the large pores. When comparing the yield of different network geometries with the same ϕ^* and D_0, it becomes apparent that the largest gains from geometric optimization are also found in the range of very fast macropore transport (large D_0). This is expected, because fast macropore access has the most potential to reduce overall diffusion resistance, when used efficiently.

A sensitivity analysis of the optima shows that the network geometry can vary substantially without affecting production in a major way. The geometric optima are therefore rather shallow. The geometry of the outside layer is most important because it gives the bulk of the production. Therefore, it is specified unambiguously by the optimization, whereas the shape of inner layers can vary to some extent. Typically, a 2% change in the position or size of the outermost channels can change production by as much as 10%, whereas a 50% change in the size of the central channel produces an insignificant 2% change in the overall yield. This shallowness of the optima is in itself a challenge for the optimization routines.

Knudsen diffusion regime

In this section, Knudsen diffusion is considered as the dominant transport mechanism in the large pore network. This assumption is correct only for pores with a cross section up to 50 nm, so it is somewhat questionable to consider that all large pores in our model pellet are in this regime. Still, the analysis with pure Knudsen diffusion adds insight to the problem of geometric optimization. In the Knudsen regime, the diffusivity in the pores is proportional to the pore diameter d_i: $D_{0i}=(d_i/L)\,D_K$. The proportionality factor D_K may include pore roughness effects (Malek and Coppens, 2001). Because the Knudsen diffusivity is pore-size dependent, changes in geometry have a more pronounced effect on yield, and as a consequence, optima are *less shallow* than in the molecular diffusion regime, and there is a much higher gain in production by optimization.

Figure 1b shows that the pore-size distribution of optimized networks is much broader than that of the networks in the molecular diffusion regime, under comparable conditions (Figure 1a). Large pores offer a clear advantage in the Knudsen diffusion regime, but increasing the size of all pores would increase porosity too much. In the optimal networks, a tradeoff is realized by keeping most channels small, whereas having a few very large pores. Optimal Knudsen networks are typically hierarchical, with larger pores servicing smaller pores, and they feature a radial porosity gradient very much like their counterparts in the previous section. The network in Figure 1b, center ($\phi^* = 10\sqrt{10} \approx 31.6$), is very close to being self-similar.

Intermediate diffusion regime

In reality, both Knudsen and molecular diffusion will occur simultaneously in pores. To make the model more realistic, the molecular and Knudsen diffusivities were combined with Bosanquet's formula, which is a good approximation for binary mixtures and equimolar counterdiffusion

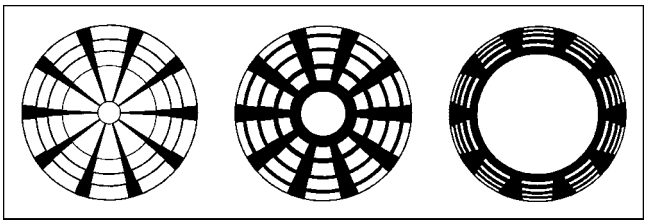

Figure 2. Optimal geometry of circular networks.

Pores are black microporous catalytic support is white. From left to right, $\phi^*=10$, 31.6, 100. Molecular diffusion in the large pores, $D_0/D_e=10^2$.

$$\frac{1}{D_{0i}} = \frac{1}{D_0} + \frac{1}{D_K(d_i/L)} \tag{4}$$

Typical pore diffusivities for dilute gases at industrially relevant pressures and temperatures give simulation parameters on the order $D_0/D_e \sim 10^2$ and $D_K/D_e \sim 10^3$, although these values may vary over a broad range. The smallest pores of the large-pore network fall in the Knudsen regime (mesopores), whereas transport through the larger ones is dominated by molecular diffusion (macropores up to 1 μm in a 20 μm particle). Optimal networks derived for this range of parameters are shown in Figure 1c. They are clearly intermediate in character between the optimal networks obtained for molecular diffusion and those obtained in the Knudsen regime, showing the affinity toward a broader pore-size distribution of the latter.

Optimization within other Classes of Symmetry

Networks of circular symmetry

Although facilitating the global optimization and revealing some key features of optimal networks, the precept of square pellet geometry introduces some artificialities as well. First, there is no angular symmetry, so that corners are favored production-wise over central edge sections, because of their larger exposure. Second, because channels have a fixed width as they pass through the pellet, the porosity cannot change in a natural way from the pellet center to the outside. These problems make the interpretation of the optimal network results less transparent. To overcome some of the geometric artificiality, calculations were repeated for a circular nanoporous pellet with a network of radial ("wedge") and concentric ("ring") high-diffusivity channels (Figure 2). Optimal circular pore networks are found to have the same qualitative properties as the square ones. For fast reactions ($\phi^* = 100$), an eggshell structure is formed again: the outside layers matter most; an increased surface area near the pellet surface is achieved by arranging the outside layers as thin, closely spaced onionskins. This is not the optimal configuration for slower reactions, where the layers have a comparable thickness, and there is only a small radial porosity gradient with a larger porosity of the outside layers to facilitate penetration to the core.

Tree-like pores

To further depart from the geometric constraints of the previous sections, a very general problem was studied, in the form of a single branched macropore near the surface of the pellet. The size and position of the branches, as well as the

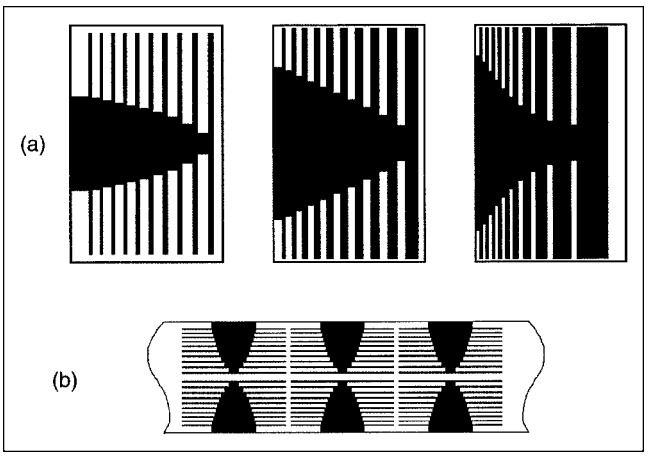

Figure 3. (a) Optimal geometry of branched pores.

Pores are black microporous catalytic support is white. From left to right, $\phi^*=10$, 31.6, 100. Molecular diffusion in the large pores, $D_0/D_e=10^2$. (b) Periodic arrangement of optimal pores in a slab.

radius of the main pore, are variable and subject to optimization. To keep the problem even more general, the radius of the main pore is allowed to vary between consecutive branching points. If reaction is limited to the pore walls, the conversion of such a structure can be computed analytically, but here the pores are carved into a permeable, microporous material, with an effective diffusivity D_e, which makes computation significantly more complicated. Molecular diffusion with diffusivity $D_0 \gg D_e$ is considered the main transport mechanism in the pore tree, and reflecting boundary conditions are set on the lateral walls, hinting at the existence of identical neighboring pores (the pore is part of a periodically extended catalyst slab, Figure 3b). Examples of optimal tree-like pore structures are shown in Figure 3a. Again, the optimal porosity increases with increasing diffusion limitations, but the optimal porosity *profile* is also changing with ϕ^*. For fast reaction, the outside layers are again densely packed in an "eggshell", but now the tradeoff between production in the outside layers and ease of access to the internal layers is more clearly seen.

Optimization of self-similar, fractal-like catalysts

As earlier stated in the introduction, self-similar fractal pore hierarchies are in principle good candidates for optimal networks, as suggested by many other authors. On the basis of the optimal network structures computed so far, this study aims to make a significant step forward in this debate, by actually comparing the performance of the optimal networks with that of fractal-like, hierarchical networks. To assess the potential advantages of fractal-like constructions, the performance of a fractal-like catalyst is also compared to that of a network with uniform spatial distribution of the catalyst. The former is a hierarchical, prefractal object constructed iteratively from downscaled copies of itself, whereas the latter features a grid-like network of large pores of the same size. Under these assumptions, the uniform network models a material with a bidisperse pore-size distribution, whereas the fractal-like material contains a broad, power-law pore-size distribution. Macropore diameter scales as $d_n = d_0/\lambda^n$, where d_0 is the central pore size, λ is the similarity ratio, and n is the level or "generation" of the fractal construction. As before, the reactive regions are nanoporous, described as an effective medium with diffusivity D_e, and are separated by large pores of diffusivity $D_{0i} \gg D_e$. The investigation closely parallels the work of Gavrilov and Sheintuch (1997), with the exception of the optimization aspect, which is new. It also extends the approach of Gavrilov and Sheintuch by considering nanoporous instead of nonporous channel walls, and solving for the complete 2-D concentration field. The two calculation schemes coincide only in the range of very large ϕ^* and D_0.

Comparison at fixed porosity

First, the production of two networks having the *same number of pores* and *same porosity* ($\epsilon = 0.58$ was chosen for illustration) is compared for the same process parameters. The two networks have the same number, size, and shape of reactive regions ("building blocks"). Any difference in production is solely because of the different spatial allocation of reactive zones – a purely geometric effect. The larger central pores of the fractal-like network facilitate fast transport to the inside of the pellet, at the expense of having higher-generation channels that are narrower than those of the uniform network.

When molecular diffusion is the dominant pore transport mechanism, the difference in yield or effectiveness factor η (which is equivalent, because ϵ is the same) between the two types of materials is generally negligible. This makes sense: the overall diffusion rate is roughly the same, because the porosity is constant and the diffusivity is pore size independent. Overall, fractal-like networks perform marginally better than the uniform ones, a reflection of lower transport limitations in the central pores of the fractal-like network. The difference is of the order of a few percent (max. 5% in a 5th generation or 31 $\times$ 31 pore-network with $D_0/D_e=10^2$, under realistic process parameters).

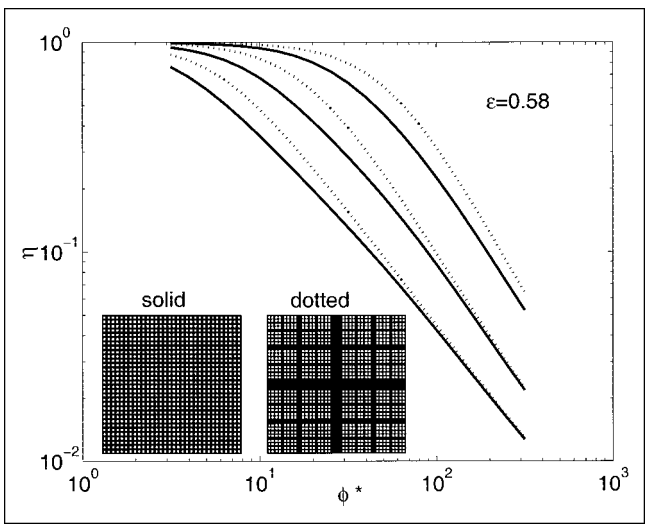

Figure 4. Effectiveness factor η of a 5th generation fractal-like (dotted line), and uniform (solid line) network of the same porosity (0.58), in the Knudsen diffusion regime.

From top to bottom, $D_K/D_e=10^4$, 10^3, 10^2.

When Knudsen diffusion is considered in the meso/macropores, the behavior is qualitatively similar (Figure 4). Quantitatively, the difference is significant, with the self-similar network producing up to 40% more than its uniform counterpart (result based on a 5th generation network with $D_K/D_e=10^3$). The difference again reflects the more efficient transport in the large pores of the fractal-like network, and could be even more important in a diffusion regime in which D_0 would depend even more strongly on pore size (for example, configurational diffusion).

For both leading transport mechanisms, this difference in yield is also found to increase with increasing size and complexity of the hierarchical network. This can be explained by the fact that when the number of generations of the fractal construction increases, the advantage of fast access is preserved deeper into the pellet, whereas diffusion limitations become acute only at the smallest scales of the construction.

One important outcome of this calculation is that, for both molecular and Knudsen diffusion, the advantages of the fractal-like networks over the uniform grid-like ones manifest only in the range of *moderate* diffusion limitations (shoulder of the η–ϕ^* curve). This observation disproves a common belief that fractal-like structures should prevail exclusively in the range of *strong* diffusion limitations. These results can be explained as follows. In the case of very low diffusion limitations, the structure of the large-pore network is irrelevant. However, at very large ϕ^*, for realistic values of channel diffusivity virtually the entire pellet interior is screened, so all the production occurs on the pellet skin, and the structure of the core is again irrelevant. In both cases, there is no reason why a self-similar network would yield anything but marginal benefits over a uniform one with the same porosity. The advantages of the former one are therefore in the intermediate regime, where there is enough, yet incomplete penetration of the pellet core.

Optimization of fractal-like networks and comparison with global optima

In the next computation phase, the porosity ϵ of the networks becomes an additional target for optimization. Although the earlier comparison answered the question: "Which structure is more efficient with a given amount of catalyst?" now the question is "Which geometry is more efficient within a given volume (catalyst plus pores)? " Now an optimum is sought within each of the two classes of restricted network geometries, and the optimal fractal-like network is compared with the optimal uniform one, and then with the overall optimal ones (unconstrained geometry) computed in previous sections.

Again, when molecular diffusion dominates transport in the macropores, conversion rates of optimal fractal-like networks are marginally better than those of optimal uniform networks in the range of moderate diffusion limitations ($<5\%$ for a 31×31 pore network, $D_0/D_e=10^2$). In the Knudsen diffusion case, the same qualitative behavior is found, but the difference in performance between optimal self-similar and optimal uniform networks is more significant ($\sim 40\%$ for a 31×31 pore network, $D_K/D_e=10^3$, $\phi^*=100$).

It is remarkable that a completely different picture emerges when the data is visualized in terms of effectiveness factors. Uniform and self-similar networks have different optimization strategies, which usually lead to different optimal porosities, and consequently, significantly different effectiveness factors. Although in the self-similar structures large pores can be opened up to facilitate an efficient use of the internal surface, the same cannot be achieved in the uniform ones without sacrificing too much production volume in the outer layers. As a result, the optimal uniform networks are less porous. Therefore, in the case of molecular diffusion, for a realistic range of process parameters, the effectiveness factor of the optimal 4th generation (15×15 pores) fractal-like network is up to 25% greater than that of its uniform counterpart, *although the yields of the two are almost identical*. This performance is the result of intelligent space allocation within the self-similar network. The advantage is much more dramatic in the case of Knudsen diffusion, where optimization yields a huge boost in the effectiveness factor (the 5th generation self-similar network is up to 120% more efficient than the uniform one). The more realistic, intermediate case combining molecular and Knudsen diffusivity (Bosanquet formula) falls between. In this case, the smallest pores follow mostly Knudsen behavior, whereas the larger ones are in the molecular diffusion regime. The self-similar structure still manages to show a major advantage in the effectiveness factor η over the uniform one, by virtue of the fact that the bulk of the production takes place in the smallest pores, which are the most numerous. Therefore, the behavior is closer to that of a purely Knudsen network.

At this stage, the performance of optimal fractal-like and uniform networks was compared to that of the overall-optimal ones with the same number of pores, and the same process parameters. For all considered transport mechanisms, the latter are found to have a significantly higher yield than *both* fractal-like and uniform networks (for example, $\sim 15\%$ higher for 15×15-pore networks with molecular diffusion, $D_0/D_e=10^2$, $\phi^* = 10^2$).

Although this result seems rather disappointing, a truly remarkable fact is again revealed when the data is visualized in terms of effectiveness factors. Under the same process conditions, the effectiveness factor of the optimal fractal-like network is virtually indistinguishable from the one of the truly optimal network (Figure 5). This is true for both Knudsen and molecular pore diffusivity, and, as expected, also for the mixed diffusivity. Therefore, self-similar networks make optimal use of the available catalyst and reaction volume, in the sense that they have virtually the highest activity per unit catalyst mass in a given volume.

Sensitivity to catalyst deactivation

For all the bimodal pore networks discussed in this study, it was found that in the intermediate diffusion limitation range, the effectiveness factor varies faster than $1/\phi^*$, both in the Knudsen and in the molecular diffusion regime. Hence, the conversion varies with k slower than the classic $k^{1/2}$ behavior manifest at large k (Figure 6). This effect was observed by other researchers, who proposed the existence of an intermediate scaling regime in which the conversion rate of a fractal catalyst is less sensitive to k than that of a nonfractal one (Sheintuch, 2000; Mougin et al., 1996; Giona et al., 1996). All sources that have reported this peculiar behavior, used models that consider reaction on impermeable pore walls only. By

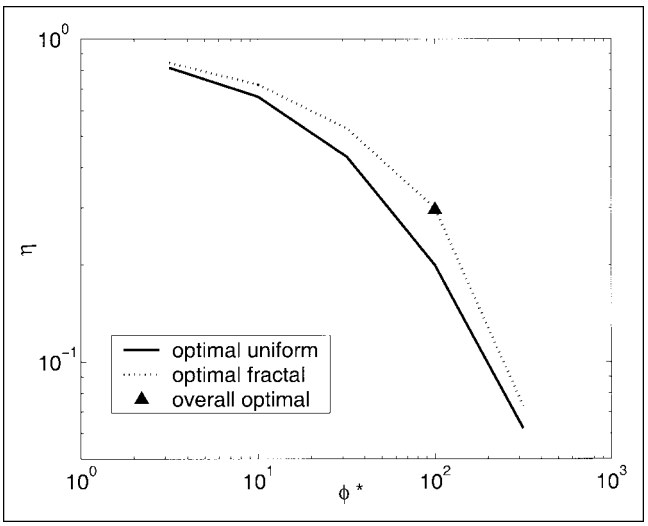

Figure 5. Effectiveness factor η of the optimal uniform (solid line), and optimal fractal-like (dotted line) network.

The overall optimum for $\phi^*=100$ is shown for comparison. Knudsen diffusion in the large pores, $D_K/D_e=10^3$.

contrast, in our model pellets, the pore walls themselves are microporous, and we find that a range of k in which the yield varies slower than $k^{1/2}$ is not only present in fractal-like networks, but also in uniform networks, as well as in networks with a random distribution of pores. We conjecture that this is true in *any* bimodal porous catalyst in which the diffusivity of the large pores is much larger than the nanopore diffusivity of the reactive regions, and under suitable porosity and process parameter requirements. In our model, the effect is more important at larger pellet porosity, and in pellets that have a large specific surface area in the outside layers.

Similar to published results, production of fractal-like structures was found to be less sensitive to variations in k than that of uniform ones, the effect being much more pronounced when Knudsen diffusion is the dominant transport mechanism. The range of k corresponding to this intermediate regime increases with increasing range of fractal scaling. This effect may prove of great relevance to catalysis. As noted already by Villermaux et al. (1987) and Sheintuch and Brandon (1989), such an intermediate scaling regime would make a fractal-like catalyst less sensitive to deactivation.

Concluding Remarks

The classical problem of first-order reaction and diffusion was studied numerically in a model of a multistructured catalyst, in which a nanoporous material is serviced by a network of large pores. The geometry of the networks was optimized so as to maximize yield. This type of unconstrained, full-scale geometric optimization of catalytic networks is new, and, thus, provides valuable insight into the optimal structure of such materials, and how they compare to fractal-like pore hierarchies and uniform, bidisperse pore networks. Because of computing limitations especially on the optimization side, the models considered were only 2-D, but the results are expected to hold identically in three dimensions, because the relevant phenomena are qualitatively the same.

For a wide range of geometry classes and process parameters, the calculated optimal networks were typically found to have a spatially nonuniform distribution of active material, with a broad pore-size distribution.

Compared to a uniform, bidisperse structure of the same porosity, gains in conversion from the optimization process are on the order of a few percent when molecular diffusion dominates transport in the large pores, and a few tens percent when Knudsen diffusion is the dominant phenomenon, for the size and complexity of the networks considered in this study. In an intermediate, mixed diffusion regime the gains can also be significant, because in a hierarchical structure the small pores (dominated by Knudsen diffusion) are also the most numerous.

Fractal-like networks of large pores were found to have higher conversion rates and less sensitivity to the intrinsic reaction rate than uniform, bidisperse pore networks in the range of moderate diffusion limitations. The difference in yield is of the order of a few percent for the size of the networks considered in the study.

However, it is important to understand that the principal advantage of self-similar networks over other geometries is not as much in absolute yield, as in the effectiveness factor. This reflects the fact that a hierarchical, self-similar network achieves optimal conversion at a relatively higher porosity; therefore, it *performs at a relatively higher effectiveness factor* than most structures. In fact, remarkably, the effectiveness factor of the optimal fractal-like catalyst was found to be indistinguishable from the one corresponding to the globally optimal structures, suggesting that fractal catalysts use the reaction volume in an almost optimal way. This result may have important practical implications for the rational design of novel catalytic materials and reactors. The structure of the truly optimal networks (Figures 1, 2, 3) is

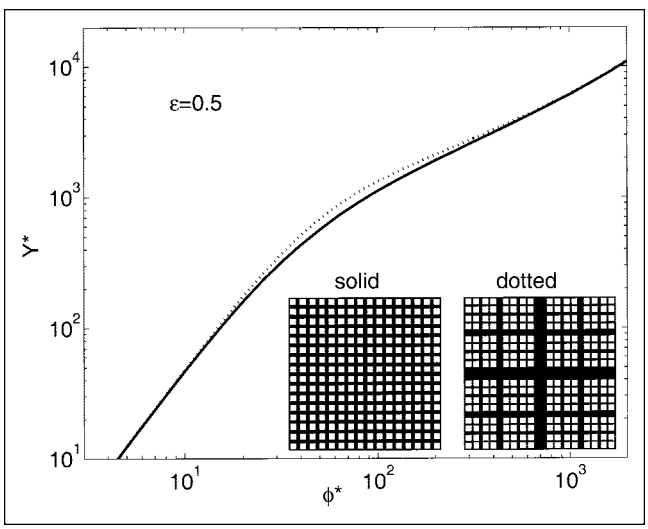

Figure 6. Dimensionless yield Y^* as a function of a modified Thiele modulus ϕ^*.

Knudsen diffusion in the large pores, $D_K/D_e=2\times10^3$. The graph shows an intermediate scaling regime, interpolating between the expected asymptotes $Y^*\sim k\sim\phi^{*2}$ (reaction control) and $Y^*\sim k^{0.5}\sim\phi^*$ (diffusion control). The rate dependence of the yield Y^* is weaker for fractal-like catalysts (dotted line).

rather complex and hard to reproduce on very small scales. By contrast, self-similar structures could in principle be built much more easily by iterative self-assembly techniques, such as templating (Coppens et al., 2001). Also, the relatively weaker dependence of conversion on the intrinsic reaction rate, could make such materials less susceptible to catalyst deactivation.

The size and complexity of pellet models considered in the study were rather limited. Because of the extreme computational cost of global geometric optimization, which grows exponentially with the number of network channels, this framework does not allow for the optimization of larger 2-D network structures (for example, 100 × 100 pores), or of 3-D networks, for the present. Nevertheless, many of the results obtained here can be extended qualitatively to larger, more complex structures.

Lessons learned from this optimization study could also potentially extend to the natural world. Even though fractal objects, such as the lung and its bronchial tree, or the vascular network of the kidney, may not be truly optimal, they may be functioning very close to the optimum. The choice of architecture is then made based on a greater ease of construction in the case of fractal objects. For example, only two basic operations – "grow" and "split" – are needed to develop a highly complex, hierarchical, self-similar structure, such as a tree (Prusinkiewicz and Lindenmayer, 1990).

Finally, the optimal 2-D multistructured systems described here may provide attractive design solutions in the area of microfluidics, microreactors for point-of-service analysis or production, and microfuel cells.

Acknowledgments

The authors are grateful for financial support from the Dutch National Foundation for Scientific Research (NWO) by way of a PIONIER grant. S. Gheorghiu is also grateful for the support of the Delft University of Technology in the form of a research fellowship.

Notation

A, B = reacting species
$c(x,y)$ = 2-D concentration field of component A, mol/m^2
C_0 = concentration of component A at the pellet boundary, mol/m^2
d_i = diameter of i-th pore, m
d_0 = diameter of central pore in fractal-like network, m
d_n = diameter of n-th generation pore in fractal-like network, m
D_e = effective diffusivity in nanoporous material, m^2/s
D_0 = molecular diffusivity in large pores, m^2/s
D_{0i} = diffusivity in the i-th large pore, m^2/s
D_K = Knudsen diffusivity in a pore of diameter L, m^2/s
k = reaction rate constant, m^2/kg cat. s
L = pellet size, m
Y = reaction yield, mol/s
$Y^*=Y/(D_eC_0)$ = dimensionless yield

Greek letters

ε = pellet porosity
ϕ = actual Thiele modulus of pellet
$\phi^*=Lk\rho/D_e$ = modified Thiele modulus
$\eta=Y/[k\rho C_0(1-\varepsilon)L^2]$ = pellet effectiveness factor
λ = similarity ratio of the fractal-like network
ρ, $\rho(x, y)$ = density of nanoporous material, kg. cat./m^2 (two dimensions)
$\phi^* = L\sqrt{k\rho/D_e}$ modified Thiele modulus
$\eta = Y/[k\rho C_0(1-\varepsilon)L^2]$pellet effectiveness factor
λ = similarity ratio of the fractal-like network
ρ, $\rho(x, y)$ = density of nanoporous material, kg. cat./m^2 (two dimensions)

Literature Cited

Andrade, J. S., Y. Shibusa, Y. Arai, and C. McGreavy, "A Network Model for Diffusion and Adsorbtion in Compacted Pellets of Bidisperse Grains," *Chem. Eng. Sci.*, **50**, 1943 (1995).
Avnir, D., D. Farin, and P. Pfeifer, "Molecular Fractal Surfaces," *Nature*, **5**, 261 (1984).
Bejan, A., and M. R. Errera, "Deterministic Tree Networks for Fluid Flow," *Fractals,* **5**, 685 (1997).
Bejan, A., "Constructal-theory Network of Conducting Paths for Cooling a Heat Generating Volume," *Int. J. Heat and Mass Transfer,* **40**, 799 (1996).
Bejan, A., *Shape and Structure, from Engineering to Nature*, Cambridge University Press, Cambridge (2000).
Coppens, M.-O., and G. F. Froment, "The Effectiveness of Mass Fractal Catalysts," *Fractals,* **5**, 493 (1997).
Coppens, M.-O., J.-H. Sun, and Th. Maschmeyer, "Synthesis of Hierarchical Porous Silicas with a Controlled Pore Size Distribution at Various Length Scales," *Catalysis Today*, **69**, 331 (2001).
Dogu, T., "Diffusion and Reaction in Catalyst Pellets with Bidisperse Pore Size Distribution," *Ind. Eng. Chem. Res.*, **37**, 2158 (1998).
Froment, G. F., and K. B. Bischoff, *Chemical Reactor Analysis and Design*, 2nd ed., Wiley, New York (1990).
Gavrilov, C., and M. Sheintuch, "Reaction Rates in Fractal vs. Uniform Catalysts with Linear and Nonlinear Kinetics," *AIChE J.,* **43**, 1691 (1997).
Giona, M., "First-order Reaction-Diffusion Kinetics in Complex Fractal Media," *Chem. Eng. Sci.,* **47**, 1503 (1992).
Giona, M., W. A. Schwalm, A. Adrover, and M. K. Schwalm, "First-Order Kinetics in Fractal Catalyst: Renormalization Analysis of Effectiveness Factor," *Chem. Eng. Sci.,* **51**, 2273 (1996).
Goldberg, E. D., *Genetic Algorithms in Searching, Optimization, and Machine Learning*, Addison Wesley, Reading (1989).
Hegedus, L. L., and C. J. Pereira, "Reaction Engineering for Catalyst Design," *Chem. Eng. Sci.,* **45**, 2027 (1990).
Keil, F. J., "Diffusion and Reaction in Porous Networks," *Catalysis Today*, **53**, 245 (1999).
Kresge, C. T., M.E. Leonowice, W. J. Roth, J. C. Vartuli, and J. S. Beck, "Ordered Mesoporous Molecular Sieves Synthesized by a Liquid Crystal Template Mechanism," *Nature*, **359**, 710 (1992).
Loewenberg, M., "Diffusion-Controlled, Heterogeneous Reaction in a Material with a Bimodal Pore Size Distribution," *J. Chem. Phys.,* **100**, 7580 (1994).
Malek, K., and M.-O. Coppens, "Effects of Surface Roughness on Self- and Transport Diffusion in Porous Media in the Knudsen Regime," *Phys. Rev. Lett.,* **87**, 125505–1 (2001).
Morbidelli, M., Gavriilidis, A., and A. Varma, *Catalyst Design: Optimal Distribution of Catalyst in Pellets, Reactors, and Membranes*, Cambridge University Press, Cambridge (2001).
Mougin, P., M. Pons, and J. Villermaux, "Reaction and Diffusion at an Artificial Fractal Interface: Evidence for a New Diffusional Regime," *Chem. Eng. Sci.*, **51**, 2293 (1996).
Pfeifer, P., and D. Avnir, "Chemistry in Noninteger Dimensions Between Two and Three. I. Fractal Theory and Heterogeneous Surfaces," *J. Chem. Phys.*, **79**, 3558 (1983).
Prusinkiewicz, P., and A. Lindenmayer, *The Algorithmic Beauty of Plants*, Springer, New York (1990).
Sahimi, M., G. R. Gavalas, and T. T. Tsotsis, "Statistical and Continuum Models of Fluid-Solid Reactions in Porous Media," *Chem. Eng. Sci.,* **45**, 1443 (1990).
Sapoval, B., J. S. Andrade, and M. Filoche, "Catalytic Effectiveness of Irregular Interfaces and Rough Pores: the Land Surveyor Approximation," *Chem. Eng. Sci.*, **56**, 5011 (2001).
Sheintuch, M., "On the Intermediate Asymptote of Diffusion-Limited Reactions in a Fractal Porous Catalyst," *Chem. Eng. Sci.*, **55**, 615 (2000).
Sheintuch, M., and S. Brandon, "Deterministic Approaches to Problems of Diffusion-Reaction and Adsorption in a Fractal Porous Catalyst," *Chem. Eng. Sci.,* **44**, 69 (1989).
Sun, J. H., J. A. Moulijn, J. C. Jansen, Th. Maschmeyer, and M.-O.

Coppens, "Alcothermal Synthesis Under Basic Conditions of an SBA-15 with Long-Range Order and Stability," *Adv. Materials*, **13**, 327 (2001a).
Sun, J. H., Z. Shan, Th. Maschmeyer, J. A. Moulijn, and M.-O. Coppens, "Synthesis of Tailored Bimodal Mesoporous Materials with Independent Control of the Dual Pore Size Distribution," *Chem. Comm.*, 2670 (2001b).
Sun, J. H., Z. Shan, T. Maschmeyer, and M.-O. Coppens, "Synthesis of Bimodal Nano-structured Silicas with Independently Controlled Small and Large Mesopore Sizes," *Langmuir,* **19,** 8395 (2003).
Villermaux, J., D. Schweich, and J. R. Authelin, "Transfert et Réaction à une Interface Fractale," *Comptes Rendus de l'Académie des Sciences,* **304**, 399 (1987).
Zhao, D., J. Feng, Q. Huo, N. Melosh, G. H. Fredrickson, B. F. Chmelka, and G. D. Stucky, "Triblock Copolymer Synthesis of Mesoporous Silica with Periodic 50 to 300 Ångström Pores," *Science*, **279**, 548 (1998).

Manuscript received Dec 18, 2002; and revision received July 10, 2003.